Mass-yield distributions of fission products in bremsstrahlung-induced fission of ^{232}Th

H. Naik
Radiochemistry Division, Bhabha Atomic Research Centre, Mumbai 400085, India

G. N. Kim* and K. Kim
Department of Physics, Kyungpook National University, Daegu 702-701, Republic of Korea

(Received 13 September 2017; revised manuscript received 11 December 2017; published 26 January 2018)

The cumulative yields of various fission products within the 77–153 mass regions in the 2.5-GeV bremsstrahlung-induced fission of ^{232}Th have been determined by using the recoil catcher and an off-line γ-ray spectrometric technique at the Pohang Accelerator Laboratory, Korea. The mass-yield distributions were obtained from the cumulative yields after charge-distribution corrections. The peak-to-valley (P/V) ratio, the average value of light mass ($\langle A_L \rangle$) and heavy mass ($\langle A_H \rangle$), and the average postfission number of neutrons ($\langle v \rangle_{\rm expt}$) were obtained from the mass yield of the ^{232}Th(γ, f) reaction. The present and literature data in the ^{232}Th(γ, f) reaction were compared with the similar data in the ^{238}U(γ, f) reaction at various excitation energies to examine the role of potential energy surface and the effect of standard I and standard II asymmetric modes of fission. It was found that (i) even at the bremsstrahlung end-point energy of 2.5 GeV, the mass-yield distribution in the ^{232}Th(γ, f) reaction is triple humped, unlike ^{238}U(γ, f) reaction, where it is double humped. (ii) The peak-to-valley (P/V) ratio decreases with the increase of excitation energies. However, the P/V ratio of the ^{232}Th(γ, f) reaction is always lower than that of the ^{238}U(γ, f) reaction due to the presence of a third peak in the former. (iii) In both the ^{232}Th(γ, f) and ^{238}U(γ, f) reactions, the nuclear structure effect almost vanishes at the bremsstrahlung end-point energies of 2.5–3.5 GeV.

DOI: 10.1103/PhysRevC.97.014614

I. INTRODUCTION

The postneutron mass and charge yield distributions of various fission products in the low energy fission of actinides provide information about the effect of nuclear structure such as the even-odd effect and shell closure proximity as well as the dynamics of descent from saddle to scission [1,2]. In the low energy fission, the mass-yield distribution of pre-actinides and heavier actinides above Cf are symmetric in nature, whereas that of actinides within U-Cf is asymmetric with double humped. On the other hand, the mass-yield distribution of lighter actinides such as Ac, Th, and Pa is asymmetric with triple humped. At higher energy, the mass-yield distribution of all actinides is expected to be symmetric. Among the various actinides, isotopes of Th, U, and Pu are of primary interest from their application in reactors. As an example, the natural and enriched uranium fuels are useful in conventional heavy and light water reactors. Similarly, ^{238}U-^{239}Pu and ^{232}Th-^{233}U are the primary fuel of fast reactor [3–5] and advanced heavy water reactor (AHWR) [6], respectively. On the other hand, ^{232}Th-^{233}U fuel in connection with ADSs (accelerator driven subcritical systems) [7–11] is one of the proposed fuels for power generation. However, the main purpose of the ADSs is to incinerate the long-lived minor actinides (^{237}Np, ^{240}Pu, ^{241}Am, ^{243}Am, ^{244}Cm) and transmute the long-lived fission products (^{93}Zr, ^{99}Tc, ^{107}Pd, ^{129}I, ^{135}Cs) to solve the problem of nuclear hazard. In all the above mentioned reactors, the yields of fission products in the neutron- and photon-induced fission of various actinides and pre-actinides are important for decay heat calculation [12] and thus for the design of reactors. Besides the above applications, the neutron- and photon-induced fission of actinides and in particular for different isotopes of Th and U are important to explain the nuclear fission mechanism. This is because the mass and charge yield distributions in the neutron- and photon-induced fission of Th and U isotopes have significant nuclear-structure effect [1,2] at low energy, which is expected to vanish at high energy. Among these two actinides, the neutron- and photon-induced fission of Th isotopes is of more interest from the point of view of their different behavior than the expected systematic, which is called the Th anomaly. The compound nucleus in the neutron-induced fission is always one mass higher than the target actinides. Thus the fission mechanism for the target nucleus is not possible to examine. This is only possible in the low energy photon-induced fission of actinides. At high energy photon-induced fission, preneutron evaporation takes place and thus multichance fission also occurs. This causes that the average mass of fissioning nucleus is lower than the mass of the compound nucleus. Thus, it is interesting to examine the mass and charge yield distributions characteristic in the photon-induced fission of ^{232}Th and ^{238}U at various energies. The generation of monoenergetic photons with high energy is a difficult task. Thus most of the photofission experiments of ^{232}Th and ^{238}U have been carried out with a wide range of bremsstrahlung end-point energies.

*Corresponding author: gnkim@knu.ac.kr

Sufficient data for the fission product yields are available in the photon-induced fission of ^{232}Th within the bremsstrahlung end-point energies of 6.44–1100 MeV [13–26] and at 3500 MeV [21]. Similarly, the data for the fission product yields are also available in the photon-induced fission of ^{238}U within the bremsstrahlung end-point energies of 6.12–3500 MeV [14–16,22,25,27–44]. This indicates that in the bremsstrahlung-induced fission of ^{232}Th, there is a big gap in between the energies of 1100 to 3500 MeV. From the existing literature data, a very good comparative study on fission product yields in the photon-induced fission of ^{232}Th and ^{238}U within the bremsstrahlung end-point energies of 6.12–80 MeV has been done by us [24,26,44]. It was observed that in both fissioning systems, the yields of fission products around mass numbers 133–134, 138–139, and 143–144 as well as their complementary products are higher than those of the other products. It was also observed that within the bremsstrahlung end-point energy of 6.12–80 MeV, the average light mass ($\langle A_L \rangle$) and heavy mass ($\langle A_H \rangle$) in the ^{232}Th(γ, f) and ^{238}U(γ, f) reactions show different trends. Besides this, the peak-to-valley ratio in the ^{232}Th(γ, f) reaction at all energies was found to be lower than that in the ^{238}U(γ, f) reaction. This is because the mass-yield distribution in the ^{232}Th(γ, f) reaction is triple humped unlike in the ^{238}U(γ, f) reaction, where it is double humped. A similar observation has also been made by Schroder *et al.* [15] in the bremsstrahlung-induced fission of ^{232}Th and ^{238}U within the end-point energies of 300–1100 MeV and by Demekhina and Karapetyan [21,42] at 3500 MeV. However, the data for fission product yields within the bremsstrahlung end-point energies of 1100–3000 MeV are not available in the ^{232}Th(γ, f) reaction unlike in the ^{238}U(γ, f) reaction [31–33] to examine the above aspects.

In view of the above facts, in the present work, we determine the cumulative yields of various fission products within the mass region of 77–153 in the 2.5-GeV bremsstrahlung-induced fission of ^{232}Th by using a recoil catcher and an off-line γ-ray spectrometric technique at Pohang Accelerator Laboratory (PAL), Korea. The data from the present work and literature in the ^{232}Th(γ, f) reaction were compared with similar data in the ^{238}U(γ, f) reaction, over the bremsstrahlung end-point energy range of 6.12–3500 MeV, to explain the different behavior of the two fissioning systems.

II. EXPERIMENTAL DETAILS

The experiment was carried out by using the 10° beam line of the 2.5-GeV electron linac of the Pohang Accelerator Laboratory (PAL) in Korea. The bremsstrahlung was produced by impinging a pulsed electron beam on a 1.0-mm-thick W target with a size of 5.0 cm × 5.0 cm. The W target is located at a distance of 38.5 cm from the electron beam-exit window. A known amount (74.2–111.3 mg) of ^{232}Th metal foil having a thickness of 0.025 mm and area of 0.25 cm^2 was wrapped with a 0.025-mm-thick aluminum foil (purity >99.99%). The Al wrapped Th sample was fixed on a stand in air at a distance of 24 cm from the W target and positioned at 0° with respect to the direction of the electron beam. The aluminum wrapper acts as a catcher for the fission products recoiling out from the ^{232}Th metal foil during the irradiation. A schematic diagram (sketch) of the experimental setup for the bremsstrahlung production and irradiation facility at PAL is shown in Fig. 1.

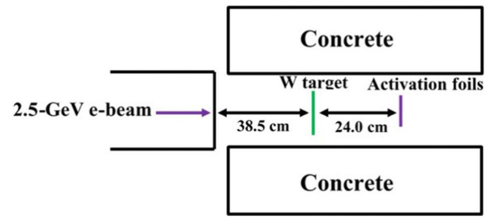

FIG. 1. A schematic diagram of the experimental setup for the bremsstrahlung production and irradiation facility of 2.5-GeV electron linac at PAL.

The target assembly was irradiated for 0.5–1.5 h with the bremsstrahlung end-point energy of 2.5 GeV. During the irradiation, the electron linac was operated with a repetition rate of 10 Hz, a pulse width of 1 ns, and electron energy of 2.5 GeV. The irradiated target assembly was cooled for 0.5–0.9 h and then taken out for γ-ray counting [22–26] of the fission products. The aluminum wrapped ^{232}Th metal foil was taken out from the irradiated assembly and mounted on a Perspex plate (acrylic glass, 1.5 mm thick) [22–26]. The Al wrapped ^{232}Th metal foil contains primarily fission products from the ^{232}Th(γ, f) reaction along with some of the products from the ^{232}Th(γ, x) and ^{27}Al(γ, x) reactions. The γ-ray activities of the fission and reaction products were measured by keeping the mounted sample on a fixed shelf of the Perspex stand attached to a precalibrated HPGe detector coupled to a PC-based 4-K-channel analyzer. The HPGe detector was a p-type coaxial CANBERA detector of 3-in. diameter × 3-in. length. The energy resolution of the HPGe detector was 2.0 keV full width at half maximum at a 1332.5-keV γ-ray peak of ^{60}Co. The efficiency of the detector system during the γ-ray counting was 20%. The standard source used for the energy and efficiency calibration was a ^{152}Eu, having γ rays in the energy range of 121.8–1408.0 keV. The standard ^{152}Eu source was used to avoid the complexity from so many other standard sources with one or few γ lines in each. The dead time of the detector system during γ-ray counting was always kept less than 10% by placing the sample at a suitable distance from the end cap of the detector to avoid pileup effects. The γ-ray counting of the sample was done in live time mode and was followed as a function of time for, at least, three half-lives for major fission products.

III. DATA ANALYSIS

A. Determination of average excitation energy

The average excitation energies ($\langle E^*(E_e) \rangle$) of the ^{232}Th(γ, f) and ^{238}U(γ, f) reactions at various bremsstrahlung end-point energies were calculated by using the following relation [36]:

$$\langle E^*(E_e) \rangle = \frac{\int_{E_{\rm th}}^{E_e} \phi(E_e, E_\gamma)\sigma_F(E_\gamma)E_\gamma dE_\gamma}{\int_{E_{\rm th}}^{E_e} \phi(E_e, E_\gamma)\sigma_F(E_\gamma)dE_\gamma}, \quad (1)$$

where the $\phi(E_e, E_\gamma)$ is the photon flux with a photon energy E_γ produced from the incident electron to the bremsstralung end-point energy, i.e., electron beam energy (E_e), $\sigma_F(E_\gamma)$ is the fission cross section as a function of the photon energy (E_γ), and $E_{\rm th}$ is the threshold energy of the fission reaction.

The bremsstrahlung spectrum $\phi(E_e,E_\gamma)$ corresponding to the bremsstralung end-point energy (E_e) was calculated using the GEANT4 computer code [45]. The photon-induced fission cross section of ^{232}Th and ^{238}U as a function of monoenergetic photon from the threshold energy to 3779 MeV are available in EXFOR [46] based on the experimental works of various authors [47–53]. From these data, it is seen that in the photofission cross sections of ^{232}Th and ^{238}U, there are two resonance peaks around 14.5 and 350 MeV. The first resonance cross sections around 14.5 MeV for the ^{232}Th(γ, f) and ^{238}U(γ, f) reactions are 64 and 175 mb, respectively. Similarly, the second broad resonance cross sections around 350 MeV for the ^{232}Th(γ, f) and ^{238}U(γ, f) reactions are 57 mb and 100, respectively. On the other hand, at the highest photon energy of 3779 MeV, the ^{232}Th(γ, f) and ^{238}U(γ, f) reaction cross sections are around 9 and 18 mb, respectively. Thus the excitation energies for various bremsstrahlung end-point energies in the ^{232}Th(γ, f) and ^{238}U(γ, f) reactions were calculated by using the experimental photofission cross sections from literature [47–53] and the simulated bremsstrahlung spectrum from the GEANT4 computer code [45]. The calculated average excitation energies ($\langle E^*(E_e)\rangle$) of the ^{232}Th(γ, f) and ^{238}U(γ, f) reactions for various bremsstrahlung end-point energies are given in their respective tables or used in the figures of interest.

B. Determination of yields for fission products

The spectrum analysis was done by using the program Gamma Vision 5.0 (EG&G Ortec). The photopeak areas of different γ rays for the fission products of interest were obtained by subtracting the linear Compton background from their net photopeak areas. From the observed number of γ rays ($N_{\rm obs}$) under the photopeak of each individual fission product, their cumulative yields ($Y_{\rm R}$) relative to ^{92}Sr were calculated by using the standard decayequation [22–26],

$$Y_R = \frac{N_{\rm obs}({\rm CL/LT})\lambda}{\left[\int_{E_b}^{E_e} n\sigma_F(E_\gamma)\phi(E_e,E_\gamma)dE_\gamma\right] I_\gamma \varepsilon(1-e^{-\lambda t_{\rm irr}})e^{-\lambda t_{\rm cool}}(1-e^{-\lambda {\rm CL}})}, \tag{2}$$

where n is the number of target atoms and σ_F (E_γ) is the photofission cross section of the target nuclei as a function of photon energy. $\phi(E_e,E_\gamma)$ is the photon flux, E_b is the fission barrier [54], E_e is the bremsstrahlung end-point energy, I_γ is the abundance or branching intensity of the γ ray, ε is the detection efficiency of the γ ray in the detector system, and λ is the decay constant of the fission product of interest ($\lambda = \ln 2/T_{1/2}$). The $t_{\rm irr}$ and $t_{\rm cool}$ are the irradiation and cooling times, whereas CL and LT are the clock (real) time and the live time of counting, respectively. The nuclear spectroscopic data, such as the γ-ray energies, the half-lives ($T_{1/2}$), and the branching intensities of the fission products were taken from the literature [55–57]. In Eq. (2), the photofission cross section [$\sigma_F(E_\gamma)$] is the main deciding factor for the independent yields of fission products and thus their cumulative yields [21,42].

The cumulative yields ($Y_{\rm R}$) of the fission products relative to the fission-rate monitor ^{92}Sr were calculated using Eq. (2). Their relative mass yields (Y_A) were calculated by using Wahl's prescription of charge distribution [58]. The fractional cumulative yield ($Y_{\rm FCY}$) of a fission product in an isobaric mass chain is given as follows:

$$Y_{\rm FCY} = \frac{{\rm EOF}^{a(Z)}}{\sqrt{2\pi}{\sigma_z}^2}\int_{-\infty}^{Z+0.5}\exp\left[-(Z-Z_P)^2/2{\sigma_z}^2\right]dZ, \tag{3}$$

$$Y_A = Y_R/Y_{\rm FCY}, \tag{4}$$

where Z_P is the most probable charge and σ_z is the width parameter of an isobaric-yield distribution. ${\rm EOF}^{a(Z)}$ is the even-odd effect with $a(Z) = +1$ for even-Z nuclides and -1 for odd-Z nuclides.

In an isobaric mass chain, it is necessary to have knowledge of Z_P, σ_z and ${\rm EOF}^{a(Z)}$ to calculate the $Y_{\rm FCY}$ value of a fission product and a mass yield (Y_A). The ${\rm EOF}^{a(Z)}$ is not expected at high energy fission. On the other hand, in the photon-induced fission of ^{232}Th [59] and ^{235,238}U [60,61], the average width parameter ($\langle\sigma_z\rangle$) increases from 0.56 ± 0.06 at the bremsstrahlung end-point energy of 6.1-14 MeV to 0.72 ± 0.06 at 20–30 MeV. Similarly, Umezawa *et al.* [62] have shown that in the medium energy proton- and α-induced fission of ^{232}Th and ^{238}U, the average width parameter ($\langle\sigma_z\rangle$) is 0.70 ± 0.06. In view of this, in the present work, we have used the $\langle\sigma_z\rangle$ value of 0.75 in Eq. (2) for calculation of $Y_{\rm FCY}$ values of the individual fission products in the 2.5-GeV bremsstrahlung-induced fission of ^{232}Th. The justification for using the $\langle\sigma_z\rangle$ value of 0.75 is given below.

The Z_P values of individual mass chain (A) in the ^{232}Th(γ, f) reaction can be calculated by using the prescription of Umezawa *et al.* [62]. However, in their prescription [62], calculation of Z_P values need the most probable charge based on the unchanged charge-density distribution ($Z_{\rm UCD}$) [63] and the charge polarization parameter (ΔZ). The calculation of $Z_{\rm UCD}$ needs exact idea of pre-scission ($\nu_{\rm pre}$) and postscission ($\nu_{\rm post}$) neutrons. The $\nu_{\rm pre}$ value can be calculated based on their prescription by using the exact excitation energy. The exact average excitation energy can only be obtained after multichance fission correction. In the case of bremsstrahlung-induced fission the calculation of the exact average excitation energy is not so simple due to the bremsstrahlung spectrum in addition to multichance fission for all light masses fissioning nuclei for the same compound nucleus. So calculating the prescission neutrons by taking only the average excitation energy of compound nucleus without considering the multichance fission will not give a proper value. This is because the fission cross section given in the literature is only for the ^{232}Th(γ, f) and ^{238}U(γ, f) reactions but not for the light masses fissioning nuclei of the same elements. The calculation of the ν_{post} value as a function of the fission product mass number has also been given in the prescription of Umezawa *et al.* [62]. However, in their [62] prescription the ν_{post} value of a particular mass for all excitation energy was assumed to be the same, which is not valid at higher excitation energy. The neutron emission as a function of mass for the fission fragment in the bremsstrahlung-induced fission was also obtained by Strecker *et al.* [64] only at the low energy region and thus not valid in the higher energy of the present work.

In order to avoid all these limitations, the most probable charge (Z_P) and the average width parameter ($\langle\sigma_z\rangle$) for different mass chains were calculated based on the relation used by Deppman *et al.* [65]. The fission yields in 50- and 3500-MeV bremsstrahlung-induced fission of ^{232}Th [21] and ^{238}U [42] have been published by Demekhina and Karapetyan [21,42]. On the other hand, Deppman *et al.* [65] have done an analysis of the fission product yields in 50- and 3500-MeV bremsstrahlung-induced fission of ^{232}Th [21] and ^{238}U [42] by using the simulation code CRISP [66]. In their calculations, it was possible to obtain the isobaric charge distribution parameters such as the most probable charge (Z_p) and corresponding width parameter (Γ_Z). According to them [65], the parameters Zp and Γ_Z ($2\sigma_Z^2$) can be represented as a linear function of the mass number of fission products (A):

$$Z_P = \mu_1 + \mu_2 A, \tag{5}$$

$$\Gamma_Z = \gamma_1 + \gamma_2 A, \tag{6}$$

where μ_1,μ_2,γ_1, and γ_2 are the different coefficients [65], whose values are described below.

As shown by Deppman *et al.* [65], the experimental values of μ_1 and μ_2 in the ^{238}U(γ, f) reaction are 5.70 $\pm$ 0.60 and 0.356$\pm$0.005 at the bremsstrahlung end-point energy of 50 MeV, whereas at 3500 MeV, they are 5.32 $\pm$ 0.62 and 0.362 $\pm$ 0.005, respectively. Similarly, the experimental values of μ_1 and μ_2 in the ^{232}Th(γ, f) reaction are 3.89 $\pm$ 0.67 and 0.371 $\pm$ 0.005 at the bremsstrahlung end-point energy of 50 MeV, whereas at 3500 MeV, they are 4.14 $\pm$ 0.70 and 0.356 $\pm$ 0.005, respectively. Deppman *et al.* [65] also shown that the calculated values of Γ_Z in the ^{238}U(γ, f) reaction are 1.03 $\pm$ 0.12 and 1.09 $\pm$ 0.13 at the bremsstrahlung end-point energies of 50 and 3500 MeV based on the values of $\gamma_1 = 0.92$ and $\gamma_2 = 0{,}003$, respectively. Similarly, the calculated values of Γ_Z in the ^{232}Th(γ, f) reaction are 1.13 $\pm$ 0.14 and 1.14 $\pm$ 0.15 at the bremsstrahlung end-point energies of 50 and 3500 MeV based on the values of $\gamma_1 = 0.59$ and $\gamma_2 = 0.005$, respectively. Thus in the present work, we have used the μ_1 and μ_2 values as 4.0 and 0.362 in the ^{232}Th(γ, f) reaction at the bremsstrahlung end-point energy of 2500 MeV for the calculation of the Z_P values. Similarly, we have considered the Γ_Z value of 1.135, which corresponds to the $\langle\sigma_z\rangle$ value of 0.753. Deppman *et al.* [65] have also mentioned that the width parameter ($\Gamma_Z = 2\sigma_Z^2$) is practically independent of A. Thus, we have used the σ_Z value of 0.75 for all isobaric mass chains, which is the same value based on the prescription of Umezawa *et al.* [62]. The Z_P values as a function of mass number and the average width parameter ($\langle\sigma_z\rangle$) of 0.75 were used in Eq. (2) to calculate the Y_{FCY} for different mass chains. The mass yield (Y_A) of the fission products from their relative cumulative yield (Y_{R}) was obtained from Eq. (3) by using the Y_{FCY} values of different fission products. The relative mass yields of the fission products obtained as mentioned above were normalized to a total yield of 200% to obtain the absolute mass yields. The absolute cumulative yields of the fission products in the 2.5-GeV bremsstrahlung-induced fission of ^{232}Th were obtained by using the mass-yield data and Y_{FCY} values.

The relative cumulative yield (Y_{R}) and mass yield (Y_A) of the fission products in the 2.5-GeV bremsstrahlung-induced fission of ^{232}Th along with the nuclear spectroscopic data from literature [55–57] are given in Table I. The absolute cumulative yields and the mass yields in the above fissioning system from the present work also are given in the last two column of Table I. The uncertainty shown in the measured cumulative yield of individual fission products in Table I is the statistical fluctuation of the mean value from two determinations. The overall uncertainty represents the contributions from both random and systematic uncertainties. The random uncertainty in the observed activity is due to counting statistics and is estimated to be 5–10%, which can be determined by accumulating the data for the optimum period of time, depending on the half-life of the nuclide of interest. Conversely, the systematic uncertainties are due to the uncertainties in irradiation time (0.5%), detector efficiency calibration ($\sim$3%), half-life of the fission products ($\sim$1%), and γ-ray abundance ($\sim$2%), which are the largest variation in the literature [55–57]. The overall systematic uncertainty is about 3.8%. An upper limit of uncertainty of 6.3–10.7% was determined for the fission-product yields based on the respective systematic and random uncertainties of 3.8% and 5–10%, respectively.

IV. DISCUSSION

The mass yields of fission products in the 2.5-GeV bremsstrahlung-induced fission of ^{232}Th are determined for the first time, which has been shown in Table I. The mass-yield data in the ^{232}Th(γ, f) reaction at 2.5 GeV from the present work and those at 10 and 80 MeV from our earlier work [22,24] are plotted in Fig. 2. It can be seen from Fig. 2 that there is a well-known third peak around the symmetric mass region in the mass-yield distribution of 10, 80, and 2500 MeV bremsstrahlung-induced fission of ^{232}Th. In particular, the highest yield of symmetric product in the ^{232}Th(γ, f) reaction at 2.5 GeV is clearly seen around mass number of 113–114. It can also be seen from Fig. 2 that even at 2.5 GeV, the mass-yield distribution in the ^{232}Th(γ, f) reaction is asymmetric in nature. Similarly, a triple humped mass-yield distribution in the high energy bremsstrahlung-induced fission of ^{232}Th was also observed by Schroder *et al.* [15] at 300–1100 MeV and by Demekhina and Karapetyan [21] at 3500 MeV. However, Deppman *et al.* [65] in their theoretical calculations were not able to reproduce the experimental triple humped mass-yield distributions [21] in the ^{232}Th(γ, f) reaction. In the high energy bremsstrahlung-induced fission of ^{238}U, an asymmetric mass-yield distribution with a double hump was observed by Schroder *et al.* [15] at 300–1100 MeV, by Komar *et al.* [32] at 1000 MeV, by David *et al.* [33] at 1800–2000 MeV, and by Demekhina *et al.* [42] at 3500 MeV. Deppman *et al.* [65] in their theoretical calculations were able to reproduce

TABLE I. Nuclear spectroscopic data and the yields of fission products (%) in the 2.5-GeV bremsstrahlung-induced fission of ^{232}Th.

Nuclide	Half-life	γ-ray energy (keV)	γ-ray abundance (%)	Y_C (%)	Y_A (%)
^{77}Ge	11.3 h	264.4	54.0	0.812 ± 0.041	0.933 ± 0.047
		416.3	21.8	0.799 ± 0.030	0.918 ± 0.035
^{78}Ge	88.0 min	277.3	96.0	0.974 ± 0.099	1.337 ± 0.136
^{84}Br	31.8 min	1016.2	6.2	2.453 ± 0.129	2.541 ± 0.134
^{85}Kr^{m}	4.48 h	151.2	75.0	2.734 ± 0.084	2.747 ± 0.084
		304.9	14.0	2.567 ± 0.190	2.578 ± 0.191
^{87}Kr	76.3 min	402.6	49.6	2.356 ± 0.104	2.466 ± 0.109
^{88}Kr	2.84 h	196.3	25.9	2.479 ± 0.140	2.809 ± 0.158
^{89}Rb	15.2 min	1032.1	58.0	2.808 ± 0.096	2.860 ± 0.098
		1248.3	42.6	2.801 ± 0.099	2.852 ± 0.101
^{91}Sr	9.63 h	749.8	23.6	2.796 ± 0.176	2.814 ± 0.176
		1024.3	33.0	2.740 ± 0.129	2.758 ± 0.130
^{92}Sr	2.71 h	1384.9	90.0	2.537 ± 0.254	2.598 ± 0.260
^{93}Y	10.18 h	266.9	7.3	2.451 ± 0.114	2.456 ± 0.114
^{94}Y	18.7 m	918.7	56.0	2.253 ± 0.140	2.273 ± 0.141
^{97}Zr	16.91 h	743.4	93.0	1.857 ± 0.145	1.879 ± 0.146
^{99}Mo	65.94 h	140.5	89.4	2.217 ± 0.099	2.218 ± 0.099
		739.5	12.13	2.230 ± 0.086	2.231 ± 0.086
^{101}Mo	14.61 min	590.1	16.4	2.550 ± 0.152	2.553 ± 0.153
^{103}Ru	39.26 d	497.1	90.0	3.006 ± 0.086	3.007 ± 0.086
^{104}Tc	18.3 min	358.0	89.0	2.834 ± 0.091	2.839 ± 0.092
^{105}Ru	4.44 h	724.4	47.0	3.052 ± 0.190	3.053 ± 0.190
^{105}Rh	35.36 h	319.1	19.2	3.123 ± 0.145	3.124 ± 0.145
^{107}Rh	21.7 min	302.8	66.0	3.529 ± 0.142	3.530 ± 0.142
^{112}Ag	3.13 h	617.5	43.0	3.855 ± 0.206	3.857 ± 0.206
^{113}Ag	5.37 h	298.6	10.0	4.216 ± 0.233	4.218 ± 0.233
^{115}Cd^{g}	53.46 h	336.2	45.9	3.440 ± 0.405	3.441 ± 0.406
^{117}Cd^{m}	3.36 h	1066.0	23.1	1.284 ± 0.069	
		1097.3	26.0	1.114 ± 0.084	
^{115}Cd^{g}	2.49 h	273.4	28.0	2.659 ± 0.388	
^{115}Cd^{total}				3.859 ± 0.401	3.861 ± 0.401
^{127}Sb	3.85 d	687.0	37.0	2.227 ± 0.206	2.240 ± 0.207
^{128}Sn	59.07 min	482.3	59.0	1.449 ± 0.046	1.988 ± 0.063
^{129}Sb	4.32 h	812.4	43.0	1.687 ± 0.071	1.801 ± 0.076
^{131}I	8.02 d	364.5	81.7	1.877 ± 0.175	1.879 ± 0.175
^{132}Te	3.2 d	228.1	88.0	2.040 ± 0.122	2.213 ± 0.132
^{133}I	20.8 h	529.9	87.0	2.367 ± 0.084	2.391 ± 0.085
^{134}Te	41.8 min	566.0	18.0	1.659 ± 0.086	2.564 ± 0.133
		767.2	29.5	1.677 ± 0.112	2.592 ± 0.173
^{134}I	52.5 min	847.0	95.4	2.636 ± 0.190	2.731 ± 0.197
		884.1	65.0	2.648 ± 0.221	2.744 ± 0.229
^{135}I	6.57 h	1131.5	22.7	2.108 ± 0.089	2.334 ± 0.098
		1260.4	28.9	2.354 ± 0.104	2.606 ± 0.115
^{138}Xe	14.08 min	258.4	31.5	2.385 ± 0.099	2.703 ± 0.112
		434.5	20.3	2.296 ± 0.096	2.602 ± 0.109
^{138}Cs^{g}	33.41 min	1435.8	76.3	2.816 ± 0.129	2.829 ± 0.130
		1009.8	29.8	2.857 ± 0.122	2.870 ± 0.122
		462.8	30.7	2.834 ± 0.132	2.847 ± 0.133
^{139}Ba	83.03 min	165.8	23.7	2.826 ± 0.129	2.827 ± 0.129
^{140}Ba	12.75 d	537.3	24.4	2.935 ± 0.266	2.940 ± 0.267
^{141}Ba	18.27 min	190.3	46.0	2.357 ± 0.048	2.372 ± 0.049
^{141}Ce	32.5 d	145.4	48.0	2.938 ± 0.211	2.938 ± 0.211
^{142}La	91.1 min	641.3	47.0	2.408 ± 0.091	2.409 ± 0.091
^{143}Ce	33.03 h	293.3	42.8	2.372 ± 0.081	2.373 ± 0.081

TABLE I. *(Continued.)*

Nuclide	Half-life	γ-ray energy (keV)	γ-ray abundance (%)	Y_C (%)	Y_A (%)
^{146}Ce	13.52 min	316.7	56.0	1.992 ± 0.091	1.997 ± 0.092
		218.2	20.8	1.918 ± 0.096	1.924 ± 0.097
^{146}Pr	24.15 min	453.9	48.0	1.954 ± 0.081	1.954 ± 0.081
		1524.7	15.6	2.016 ± 0.124	2.017 ± 0.124
^{147}Nd	10.98 d	531.0	13.1	1.591 ± 0.086	1.591 ± 0.086
^{149}Nd	1.728 h	211.3	25.9	1.201 ± 0.086	1.201 ± 0.086
		270.2	10.6	1.251 ± 0.084	1.251 ± 0.084
^{153}Sm	46.28 h	103.2	30.0	0.454 ± 0.046	0.454 ± 0.046

Y_c: cumulative yields; Y_A: mass yields; ^{92}Sr: fission rate monitor.

the double humped mass-yield distributions in the ^{238}U(γ, f) reaction. However, the theoretical mass-yield distribution is broader than the experimental one [42] in the ^{238}U(γ, f) reaction. The mass-yield distributions in the 10–3500-MeV bremsstrahlung-induced fission of ^{238}U from the literature [22,27,42] are plotted in Fig. 3, The mass-yield data in the ^{238}U(γ, f) reaction at 10 MeV from the literature [22] are the absolute values. On the other hand, the mass yields in the same ^{238}U(γ, f) reaction at 100 MeV [27] are relative to ^{99}Mo, assuming its yields as 6.6%. Thus, the absolute yields were obtained by normalizing the total yields to 200% as done in the present work. In the 3.5-GeV bremsstrahlung-induced fission of ^{238}U, the values given in the literature [42] are the production cross sections in milibarns per equivalent photon. Thus, the absolute mass yields were also obtained in a similar way by normalizing the total production cross sections to 200%.

In Fig. 3, the asymmetric mass-yield distribution in the bremsstrahlung-induced fission of ^{238}U is clearly observed even at 3.5 GeV. Thus, from Figs. 2 and 3, it can be seen that even at the bremsstrahlung end-point energies of 2.5–3.5 GeV, the mass-yield distributions in the ^{232}Th(γ, f) and ^{238}U(γ, f) reactions are not symmetric. This is due to the bremsstrahlung spectrum, in which the fission contribution also comes from the low energy photons and lower mass Th and U isotopes due to prescission neutron emission. In any way, the high energy photon interaction has a different reaction mechanism than the particle-induced reactions. In the photon-induced reactions, complete energy may not be depositing in the compound nucleus and part of the energy may transmit out unlike in the particle-induced reactions, where major or full energy deposition takes place. Thus, at the same excitation energy, the mass-yield distributions in the neutron-induced fission of ^{232}Th and ^{238}U are broad and almost symmetric, whereas in the bremsstrahlung-induced fission, they still asymmetric. This fact can be observed from the fission yields data in the medium energy neutron-induced fission of ^{232}Th and ^{238}U by Ryzhov *et al.* [67] as well as in the high energy neutron-induced fission of ^{238}U by Zöller *et al.* [68]. The excitation energies are comparable in the 287-MeV neutron and 2.5-GeV bremsstrahlung-induced fission of ^{232}Th. Similarly, the excitation energies are comparable in the 235-MeV neutron and 3.5-GeV bremsstrahlung-induced fission of ^{238}U. The fission yields data are not available at the high energy neutron-induced fission of ^{232}Th to compare with the present data for 2.5-GeV bremsstrahlung-induced fission of ^{232}Th. On the other hand, at the same excitation energy, the fission yields data in the 200–260-MeV neutron-induced fission of ^{238}U show a symmetric mass-yield distribution

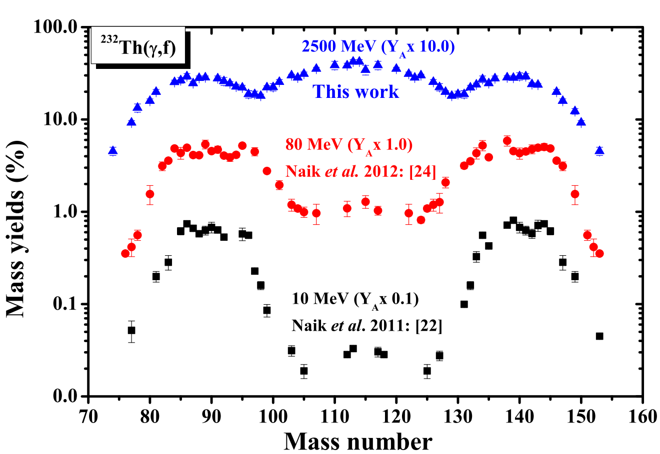

FIG. 2. Mass yields of fission products (%) as a function of mass number in the 10-, 80-, and 2500-MeV bremsstrahlung-induced fission of ^{232}Th. Mass yields for all data are multiplied by numbers written in the plot.

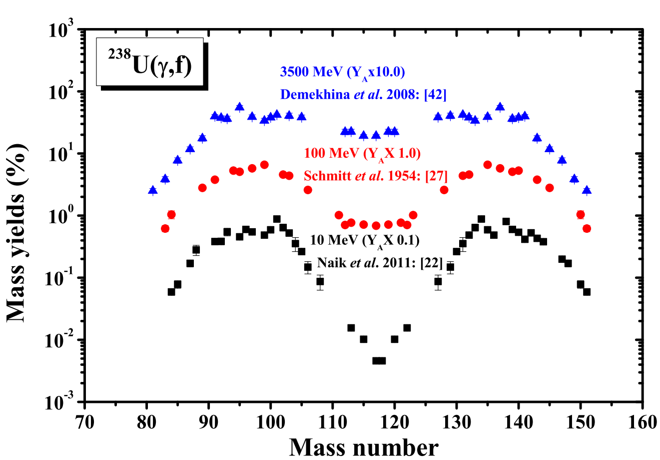

FIG. 3. Mass yields of fission products (%) as a function of mass number in the 10-, 100-, and 3500-MeV bremsstrahlung-induced fission of ^{238}U. Mass yields for all data are multiplied by numbers written in the plot.

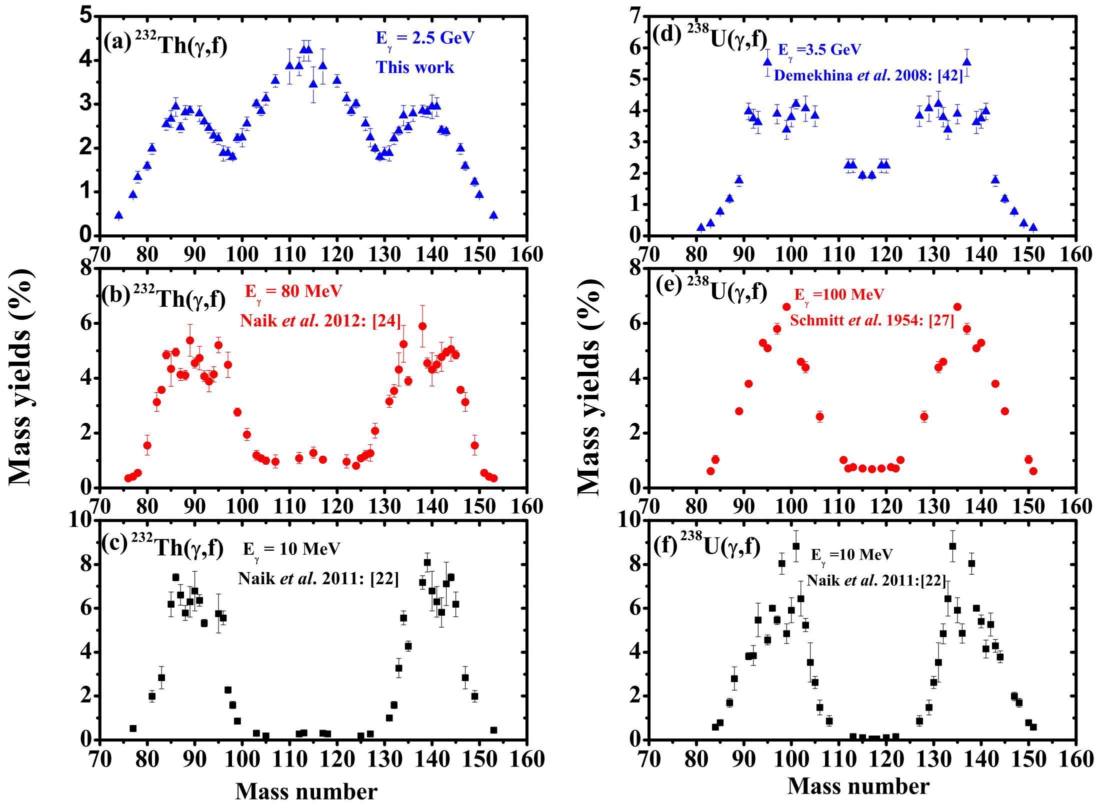

FIG. 4. Mass yields of fission products (%) as a function of mass number in the bremsstrahlung-induced fission for ^{232}Th (γ,f) with (a) $E_\gamma = 2.5$ GeV, (b) $E_\gamma = 80$ MeV, and (c) $E_\gamma = 10$ MeV and for ^{238}U(γ, f) with (d) $E_\gamma = 3.5$ GeV, (e) $E_\gamma = 100$ MeV, and (f) $E_\gamma = 10$ MeV.

[67] unlike in the 3.5-GeV bremsstrahlung-induced fission of ^{238}U [42], where it is asymmetric with double humped (Fig. 3). This observation confirms that the neutron and photon (bremsstrahlung-)induced fission mechanisms are not the same. Further, it can be seen from Figs. 2 and 3 that the fine structure in the mass-yield distribution of ^{232}Th(γ, f) and ^{238}U(γ, f) reactions decrease with increase of bremsstrahlung end-point energy. In order to examine this, the mass-yield distributions of ^{232}Th(γ, f) and ^{238}U(γ, f) reactions in the above mentioned bremsstrahlung end-point energies are shown in Fig. 4 with a linear scale.

From Fig. 4, the fine structure is clearly visible within the bremsstrahlung end-point energy of 80 MeV, but are absent at 2.5–3.5 GeV. The mass yields for the entire mass region within the bremsstrahlung end-point energies of 100–2500 MeV are not available in the literature for both the ^{232}Th(γ, f) and ^{238}U(γ, f) reactions to examine this aspect. The only mass yields within 77–153 mass region in the ^{232}Th(γ, f) reaction are available from the present work at the bremsstrahlung end-point energy of 2.5 GeV. The production cross sections of fission products in milibarns per quanta are available in the literature for the 3.5-GeV bremsstrahlung-induced fission of ^{232}Th [21] and ^{238}U [42]. As shown earlier by us [22–26,44] and others [19,20], the fine structure in the mass-yield distribution of ^{232}Th(γ, f) and ^{238}U(γ, f) reactions at the low bremsstrahlung energies are due to the higher yields of fission products around the mass region 133–134, 138–139, 143–144, and their complementary products, which is because of the even-odd effect. In order to examine this aspect, the yields of fission products for mass numbers 133–134, 139–140, and 143–144 in the ^{232}Th(γ, f) and ^{238}U(γ, f) reactions from the present work and literature data [15,21,24,27,31–33,42] above 80 MeV are shown in Table II. The yields of fission products at the bremsstrahlung end-point energies of 300–1100 MeV [15] in the ^{232}Th(γ, f) reaction is relative to ^{91}Sr, whereas in the ^{238}U(γ, f) reaction, it is relative to ^{99}Mo. Similarly, the relative yields of fission products in the ^{238}U(γ, f) reaction at the bremsstrahlung end-point energies of 48, 100, and 300 MeV are relative with respect to ^{99}Mo [27]. The relative fission product yields in the ^{238}U(γ, f) reaction at 300 MeV are available from two references [15,27]. So the relative yields from both references are normalized to obtain the mass-yield curve at 300 MeV. Similar normalization was applied for 500–1100 MeV [15] to obtain the absolute fission product yields. The absolute fission product yields in the ^{238}U(γ, f) reaction at the bremsstrahlung end-point energies of 1000, 1800, and 2000 MeV [32,33] are in arbitrary units. The absolute fission product yields for these energies were obtained after normalizing the mass-yield distribution to 200%, as done in the present work. Further, the production cross sections of fission products in milibarns per equivalent quanta are given for the ^{232}Th(γ, f) reaction at 3.5 GeV [21] and for the ^{238}U(γ, f) reaction at 1.5, 3, and 3.5 GeV [31,42]. From these data, the fission yields were obtained after normalizing the total production cross sections to 200% by following a similar procedure of the present work. The

TABLE II. Average excitation energy of compound nucleus ($\langle E^*(E_e)\rangle$), yields of the asymmetric (Y_a) fission products (%) for the mass number 133–134, 139–140, and 143–144 in the 80–3500 MeV bremsstrahlung-induced fission of ^{232}Th and ^{238}U.

Reactions	E_γ (MeV)	$\langle E^*(E_e)\rangle$ (MeV)	$A = 133-134$	$A = 139-140$	$A = 143-144$	References
	80	22.5	4.321 ± 0.602	4.555 ± 0.184	4.949 ± 0.147	[24]
			5.180 ± 0.147	4.318 ± 0.602	5.059 ± 0.440	
	300	65.6	3.115		2.259	[15]
				3.817		
	500	141	2.821		3.074	[15]
	700	171			2.135	[15]
^{232}Th(γ, f)	900	197	2.965		2.426	[15]
				3.234		
	1100	217	2.628		2.786	[15]
				3.259		
	2500	292	2.391 ± 0.085	2.827 ± 0.129	2.372 ± 0.081	this work
	3500	315	2.738 ± 0.229	2.940 ± 0.267		[21]
			3.114 ± 0.315	3.461 ± 0.346	1.307 ± 0.154	
			3.030 ± 0.246	3.091 ± 0.254		
^{238}U(γ, f)	100	22.4		4.820 ± 0.095	3.591 ± 0.425	[27]
				5.009 ± 0.095		
	300	61.3	5.617		3.294 ± 0.412	[15,27]
			4.965	5.047		
	500	112.6	5.291		3.063	[15]
	700	138.8	3.915		2.584	[15]
			3.289	4.855		
	900	156	4.374		2.770	[15]
			4.374	4.010		
	1000	162.8	4.382			[32]
					2.220	
	1100	168.9	4.198		2.519	[15]
			3.638	3.848		
	1500	188.9	3.014 ± 0.895		2.238 ± 0.448	[31]
				7.161 ± 2.387		
	1800	200	4.759 ± 0.306	3.584 ± 0.231	2.495 ± 0.259	[33]
	2000	206.3		3.026 ± 0.219		[33]
			7.855 ± 0.612			
	3000	230.8	3.418 ± 0.594		2.229 ± 0.594	[31]
				3.121 ± 0.743		
	3500	240.6	3.276 ± 0.319	3.617 ± 0.360	1.757 ± 0.178	[42]
			3.302 ± 0.233	3.257 ± 0.288		

fission yields obtained in the above ways in the ^{232}Th(γ, f) and ^{238}U(γ, f) reactions for $A = 133 - 134$, 139–140, and 143–144 within the bremsstrahlung end-point energies of 80–3500 MeV are shown in Table II. In the same table, the average excitation energies ($\langle E^*(E_e)\rangle$) calculated from Eq. (1) for different bremsstrahlung end-point energies are also given.

The data from Table II for higher energies and the other data for lower energies from literature in the ^{232}Th(γ, f) reaction [26] and ^{238}U(γ, f) reaction [44] are plotted in Fig. 5 as a function of excitation energy. The yields of fission products for the mass numbers 133, 139, and 143 were chosen due to the availability of data in a maximum number of bremsstrahlung energies. As shown by us [22–26,44] and others [20], at the lower excitation energy, the oscillating nature of the fission yield in the interval of five mass units is due to the even-odd effect. Since the N/Z ratio of the fission products is nearly 1.5, for two protons, there is an addition of three neutron numbers and thus the mass number changes by five units. Thus the higher yields of fission products for $A = 133-134$, 138–140, and 143–144 corresponding to the $Z = 52$, 54, and 56 is due to the even-odd effect. Besides this, higher yields of the fission products for $A = 133-134$ and 143–144 in even-Z fissioning systems are also due to the standard I and standard II asymmetric fission modes as mentioned by Brossa *et al.* [69] based on the shell effects [70,71]. Based on standard I asymmetry, the fissioning system is characterized by spherical heavy fragment mass numbers for $A = 133-134$ due to the spherical $82n$ shell and a deformed complementary light fragment mass. Based on the standard II asymmetry, the fissioning system is characterized by a deformed heavy fragment mass near $A = 143 - 144$ due to a deformed $86-88n$ shell and slightly deformed light fragment mass. Thus, the higher yields of fission products for $A = 133-134$ and 143–144 are due to the presence of spherical $82n$ and deformed $86-88n$ shells,

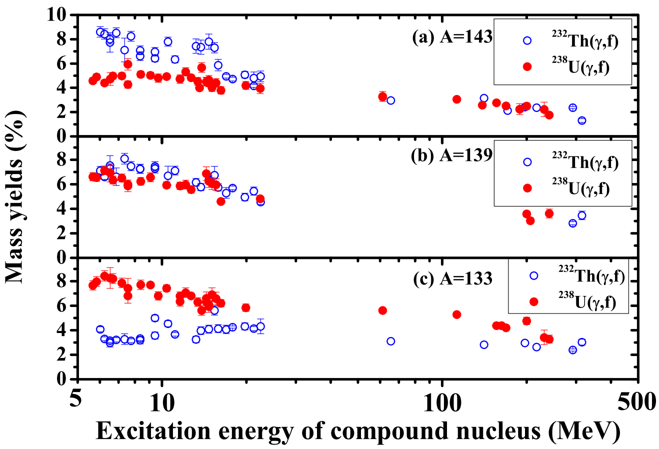

FIG. 5. Mass yields of fission products (%) as a function of excitation energy of compound nucleus for (a) $A = 143$, (b) $A = 139$, and (c) $A = 133$ in the bremsstrahlung-induced fission of ^{232}Th and ^{238}U.

respectively. The interplay of even-odd effect and shell effects in the yield profiles for $A = 133-134$, 138–140, and 143–144 corresponding to $Z = 52, 54$, and 56 changes accordingly with the neutron emission based on the excitation energy. Thus, an average $A = 139 \pm 1$, corresponding to $Z = 54$ is expected, which was shown by Schmidt *et al.* [71] in their GEF (general description of fission observables) model. At higher excitation energy, the shell effects and the even-odd effect decrease or vanish. However, the existence of feeble shell and even-odd effect even at higher excitation energy is due to the multi-chance fission. Besides this, in the bremsstrahlung-induced fission, some contribution also comes from the low energy photons and lower mass Th and U isotopes due to prescission neutron emission. Thus, the fine structure is very feeble or practically absent at the bremsstrahlung end-point energies of 2.5–3.5 GeV.

Further, it can be seen from Fig. 5 that the yield of fission products for $A = 133$ in the ^{232}Th(γ, f) reaction is low and almost remains constant or decreases very little with the increase of excitation energy. The yield for $A = 143$ is high and decreases sharply with the increase of excitation energy. On the other hand, in the ^{238}U(γ, f) reaction, it is just reversed. The yield of fission products for $A = 133$ is high and decreases sharply with the increase of excitation energy. The yield for $A = 143$ is low and decreases slowly with the increase of excitation energy. The yields of fission product for $A = 139$ in both the ^{232}Th(γ, f) and ^{238}U(γ, f) reactions are comparable and decrease slowly with the increase of excitation energy. The different trend of fission product yields for $A = 133-134$ and $A = 143-144$ in between the ^{232}Th(γ, f) and ^{238}U(γ, f) reactions cannot be explained only from the point of standard I and standard II asymmetric modes of fission [69] based on spherical $82n$ and deformed $86-88n$ shell [70] of the heavy fragments unless the shell structures of the complementary fragments are also considered. According to the scission point model of Wilkins *et al.* [70], there exists a deformed proton shell at $Z = 38$, 44, and 66 besides the spherical proton shell at $Z = 50$ and 82. Similarly, there is a deformed neutron shell at $N = 62 - 66$ and 86–88 besides the spherical neutron shell at $N = 50$ and 82. In the ^{232}Th(γ, f) reaction at low bremsstrahlung energy, there is deformed $86-88n$ shell at $A = 143-144$ and $Z = 56$, whereas its complementary light mass with $A = 86 - 84$ and $Z = 34$ has a spherical $50n$ shell. Thus the yields for $A = 143-144$ and its complementary products are higher at lower excitation energy. At higher excitation energy, the neutron evaporation causes the absence of the $50n$ shell in the complementary light mass fragment and thus the yield decreases. There is a spherical $82n$ shell at $A = 133-134$ and $Z = 52$, whereas its complementary light mass with $A \sim 96 - 94$ and $Z = 38$ has no spherical or deformed neutron shell, which causes the lower yields even at lower excitation energy. In the ^{238}U(γ, f) reaction, there is a spherical $82n$ shell at $A = 133-134$ and $Z = 52$, whereas its complementary light mass with $A \sim 102 - 100$ and $Z = 40$ has a deformed $62n$ shell. Thus the yields for $A = 133-134$ and its complementary light mass fragment have a higher yield at lower excitation energy. At higher excitation energy, the neutron evaporation causes the absence of a deformed $62n$ shell in the complementary light mass fragment and thus the yield decreases. There is a deformed $86-88n$ shell at $A = 143-144$ and $Z = 56$, whereas its complementary light mass fragment with $A \sim 92 - 90$ and $Z = 36$ has no spherical or deformed neutron shell, which causes the lower yield even at lower excitation energy.

The effect of standard I and standard II asymmetric modes of fission [69] also reflects in the average heavy mass ($\langle A_H \rangle$) and light mass ($\langle A_L \rangle$) in the mass-yield distribution of the fissioning systems. In order to examine this, the average values of light mass ($\langle A_L \rangle$) and heavy mass ($\langle A_H \rangle$) from the present work at 2.5 GeV and at other higher energy [15,21] in the ^{232}Th(γ, f) reaction as well as the similar data from literature [15,31–33,42] in the ^{238}U(γ, f) reaction are calculated from the mass yield (Y_A) of the fission products as done earlier [22–26,44] by using the following relation [37]:

$$\langle A_L \rangle = \sum (Y_A A_L) \Big/ \sum Y_A,$$
$$\langle A_H \rangle = \sum (Y_A A_H) \Big/ \sum Y_A. \tag{7}$$

The $\langle A_L \rangle$ and $\langle A_H \rangle$ values obtained using Eq. (7) in the bremsstrahlung-induced fission of ^{232}Th and ^{238}U are given in Table III. In the same table, the average excitation energies ($\langle E^*(E_e) \rangle$) calculated from Eq. (1) for different bremsstrahlung end-point energies are also given. The $\langle A_L \rangle$ and $\langle A_H \rangle$ values in the ^{232}Th(γ, f) and ^{238}U(γ, f) reactions at higher excitation energies from Table III and the similar values from the literature [26,44] at lower excitation energies are plotted in Fig. 6. It can be seen from Fig. 6 that in the ^{232}Th(γ, f) reaction, the $\langle A_H \rangle$ value decreases drastically from the value of 141 at the excitation energy of 6.02 MeV ($E_e = 6.44$ MeV) to 134 at 315 MeV ($E_e = 3.5$ GeV). This is because the fission products for $A = 143-144$ corresponding to a deformed $86-88n$ shell (i.e., the standard II configuration) are more favorable than those for $A = 133-134$ corresponding to a spherical $82n$ shell (i.e., the standard I configuration). At higher excitation energy, the deformed shell becomes weak due to neutron evaporation and thus the standard II configuration is no more favorable, which causes the sharp decrease of the

TABLE III. Average light mass ($\langle A_{\mathrm{L}}\rangle$), heavy mass ($\langle A_{\mathrm{H}}\rangle$), average excitation energy of compound nucleus ($\langle E^*(E_e)\rangle$), and the average postscission neutron numbers ($\langle v\rangle_{\mathrm{expt}}$) in the 80–3500-MeV bremsstrahlung-induced fission of ^{232}Th and ^{238}U.

Reactions	E_γ (MeV)	$\langle E^*(E_e)\rangle$ (MeV)	$\langle A_{\mathrm{L}}\rangle$	$\langle A_{\mathrm{H}}\rangle$	$\langle v\rangle_{\mathrm{expt}}$	References
^{232}Th(γ, f)	80	22.5	91.74 ± 0.25	136.75 ± 0.14	3.50 ± 0.20	[24]
	300	65.6	92.67 ± 0.43	135.33 ± 0.47	4.00 ± 0.47	[15]
	500	141	92.73 ± 0.52	135.12 ± 0.51	4.15 ± 0.52	[15]
	700	171	92.76 ± 0.56	134.95 ± 0.55	4.29 ± 0.56	[15]
	900	197	92.82 ± 0.53	134.87 ± 0.51	4.31 ± 0.53	[15]
	1100	217	92.84 ± 0.58	134.57 ± 0.58	4.59 ± 0.58	[15]
	2500	292	92.96 ± 0.57	134.05 ± 0.57	4.99 ± 0.57	this work
	3500	315	93.06 ± 0.56	133.94 ± 0.56	5.00 ± 0.56	[21][a]
	3500	315	94.00 ± 1.80	134.00 ± 2.60	4.00 ± 0.80	[21]
^{238}U(γ, f)	70	19.9	96.79 ± 0.07	137.55 ± 0.07	3.67 ± 0.11	[44]
	100	22.4	96.51 ± 0.50	137.49 ± 0.50	4.00 ± 0.50	[27]
	300	61.3	96.33 ± 0.32	137.48 ± 0.43	4.27 ± 0.43	[27]
	300	61.3	96.44 ± 0.29	137.31 ± 0.53	4.35 ± 0.53	[15]
	500	112.6	96.32 ± 0.41	137.25 ± 0.41	4.47 ± 0.41	[15]
	700	138.8	96.24 ± 0.37	137.16 ± 0.45	4.60 ± 0.45	[15]
	900	156.0	96.21 ± 0.36	136.79 ± 0.36	5.00 ± 0.36	[15]
	1000	162.8	96.22 ± 0.71	136.60 ± 0.67	5.18 ± 0.71	[32]
	1100	168.9	96.17 ± 0.41	136.63 ± 0.41	5.20 ± 0.41	[15]
	1500	188.9	96.29 ± 0.36	136.53 ± 0.54	5.18 ± 0.54	[31]
	1800	200.0	96.27 ± 0.39	136.45 ± 0.39	5.28 ± 0.39	[33]
	2000	206.3	96.23 ± 0.36	136.41 ± 0.34	5.36 ± 0.36	[33]
	3000	230.8	96.25 ± 0.50	136.24 ± 0.50	5.51 ± 0.50	[31]
	3500	240.6	96.14 ± 0.89	136.08 ± 0.68	5.78 ± 0.89	[42][a]
	3500	240.6	97.00 ± 1.70	137.00 ± 2.70	4.00 ± 1.00	[42]

[a]Present calculation from the data of Refs. [21,42] in the ^{232}Th(γ, f) and ^{238}U(γ, f) reactions.

$\langle A_H\rangle$ value with an increase of excitation energy. Accordingly, the $\langle A_L\rangle$ value increases from the value of 88 at the excitation energy of 6.02 MeV ($E_{\mathrm{e}} = 6.44$ MeV) to 93 at 315 MeV ($E_{\mathrm{e}} = 3.5$ GeV) to conserve the mass of the fissioning system. In the ^{238}U(γ, f) reaction, the $\langle A_H\rangle$ value remains almost constant or slightly decreases from the value of 137.5 at the excitation energy of 5.6 MeV ($E_{\mathrm{e}} = 6.12$ MeV) to 136 at 240.6 MeV ($E_{\mathrm{e}} = 3.5$ GeV). This is because the fission products for $A = 133-134$ corresponding to spherical 82n shell (i.e., the standard I configuration) is slightly more favorable than for $A = 143-144$ corresponding to deformed 86–88n shell (i.e., the standard II configuration). At higher excitation energy, the strong spherical 82n shell still persists due to few neutron evaporation around mass number 133–134 and thus the standard I configuration is still favorable, which causes only slight decrease of the $\langle A_H\rangle$ value with increase of excitation energy. Accordingly, the $\langle A_L\rangle$ value slightly decreases from the value of 98 at the excitation energy of 5.6 MeV ($E_e =$ 6.12 MeV) to 96 at 240.6 MeV ($E_e = 3.5$ GeV) to conserve the mas of the fissioning system. It can be seen from Fig. 6 that the $\langle A_L\rangle$ value in the ^{238}U(γ, f) reaction is always higher than that in the ^{232}Th(γ, f) reaction due to the higher mass in the former than the latter. The decrease or increase trend of the $\langle A_H\rangle$ and the $\langle A_L\rangle$ values in the ^{232}Th(γ, f) and ^{238}U(γ, f) reactions clearly indicates their dependence of excitation energy besides the role of standard I and II mode of fission [69] based on the shell effects [70] and their combinations in the complementary fragments. The above observations also indicate that the role of standard I and II mode of fission [69] are different in the ^{232}Th(γ, f) and ^{238}U(γ, f) reactions.

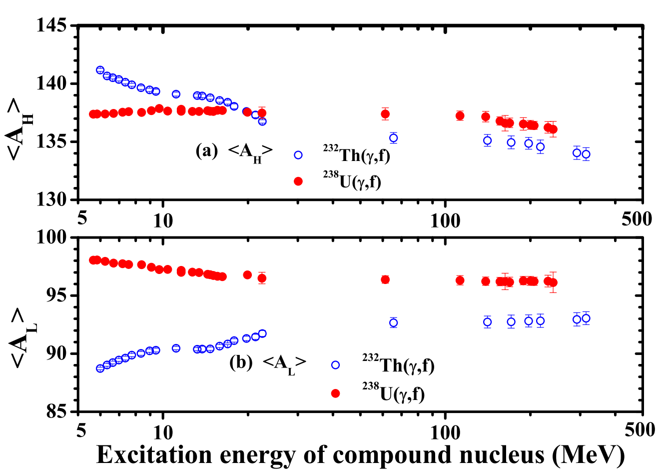

FIG. 6. (a) Average values of heavy mass ($\langle A_H\rangle$) and (b) average values of light mass ($\langle A_L\rangle$) as a function of excitation energy of compound nucleus in the ^{232}Th(γ, f) and ^{238}U(γ, f) reactions.

From the average mass of $\langle A_L\rangle$ and $\langle A_H\rangle$ as well as the compound nucleus mass (A_C), the experimental postfission average number of neutrons ($\langle v\rangle_{\mathrm{expt}}$) were calculated as follows [19]:

$$\langle v\rangle_{\mathrm{expt}} = A_C - (\langle A_L\rangle + \langle A_H\rangle). \tag{8}$$

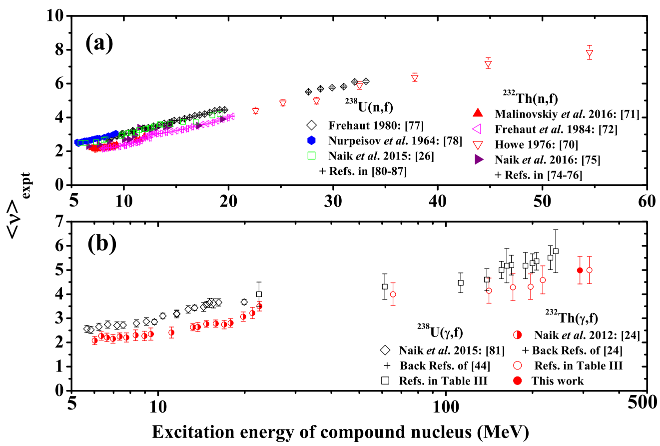

FIG. 7. The postfission average number of neutrons ($\langle v\rangle_{\text{expt}}$) as a function of excitation energy of compound nucleus in (a) the neutron- and (b) the bremsstrahlung-induced fission of ^{238}U and ^{232}Th.

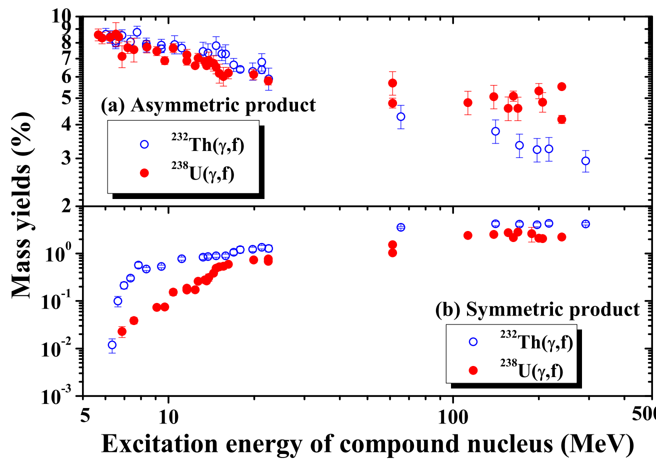

FIG. 8. Mass yields of (a) asymmetric and (b) symmetric fission products (%) as a function of excitation energy of compound nucleus in the ^{232}Th(γ, f) and ^{238}U(γ, f) reactions.

The $\langle v\rangle_{\text{expt}}$ values obtained from the bremsstrahlung-induced fission of ^{232}Th and ^{238}U at higher energies are also listed in Table III. In Table III, the average excitation energies ($\langle E^*(E_e)\rangle$) calculated from Eq. (1) for different bremsstrahlung end-point energies are also given. The postscission average number of neutrons ($\langle v\rangle_{\text{expt}}$) can also be calculated as

$$\langle v\rangle_{\text{expt}} = A_C - 2 \times A_{\text{sym}}, \tag{9}$$

where A_{sym} is the mass number of symmetric product. The symmetric products with highest yield in the 2.5-GeV bremsstrahlung-induced fission are mass numbers around 113–114. Thus the average symmetric mass (A_{sym}) of 113.5 was used in Eq. (9) for the calculation of the average number of neutrons ($\langle v\rangle_{\text{expt}}$). The postscission average number of neutrons, 4.99 ± 0.57 obtained from Eq. (8) is comparable to the value of 5 obtained from Eq. (9). The $\langle v\rangle_{\text{expt}}$ values from Table III for higher excitation energies along with the literature data [26,44] for lower energies are plotted in Fig. 7. It can be seen from Fig. 7 that the $\langle v\rangle_{\text{expt}}$ values in both the ^{232}Th(γ, f) and ^{238}U(γ, f) reactions increase with the increase of excitation energy. The $\langle v\rangle_{\text{expt}}$ value in the ^{238}U(γ, f) reaction at the same excitation energy is always higher than that of the ^{232}Th(γ, f) reaction, which is due to the increase in mass and fissility parameter. However, a similar effect on $\langle A_L\rangle$ and $\langle A_H\rangle$ values is not observed in the ^{232}Th(γ, f) and ^{238}U(γ, f) reactions.

In order to examine this aspect, the $\langle v\rangle_{\text{expt}}$ values in the ^{232}Th(n, f) and ^{238}U(n, f) reactions from literature [72–89] are plotted in the same Fig. 7 as a function of excitation energy. The excitation energies (E^*) of the ^{233}Th* and ^{239}U* compound nucleus in the neutron-induced fission of ^{232}Th and ^{238}U were calculated from the mass excess (Δ) of the target (T), neutron (n) and compound nucleus (CN) plus the neutron energy (E_n) by using the following equation:

$$E^* = (\Delta_T + \Delta_n) - \Delta_{\text{CN}} + E_n. \tag{10}$$

The mass excess (Δ) was taken from the Nuclear Wallet Cards [90]. From Fig. 7, it can be seen that the $\langle v\rangle_{\text{expt}}$ values in both the ^{232}Th(n, f) and ^{238}U(n, f) reactions increase with the excitation energy. It is also observed that at the same excitation energy, the $\langle v\rangle_{\text{expt}}$ values in the ^{238}U(n, f) reaction is higher than that in the ^{232}Th(n, f) reaction, which is due to the increase in mass and fissility parameter. This observation supports a similar effect in between ^{232}Th(γ, f) and ^{238}U(γ, f) reactions.

As shown in Figs. 2–4, the mass-yield distribution of the ^{232}Th(γ, f) reaction is triple humped and that of the ^{238}U(γ, f) reaction is double humped at the bremsstrahlung end-point energies of 2.5–3.5 GeV. However, the fine structure decreases and the yields of symmetric products increase with the excitation energy. Thus the peak-to-valley (P/V) ratio is expected to decrease with an increase of excitation energy. In order to examine this, the absolute and relative yields and the production cross sections of asymmetric and symmetric products as well as the P/V ratio from the present work and literature [15,21] in the ^{232}Th(γ, f) reaction and similar literature data [15,31–33,42] in the ^{238}U(γ, f) reaction are given in Table IV. In this table, the average excitation energies ($\langle E^*(E_e)\rangle$) calculated from Eq. (1) for different bremsstrahlung end-point energies are also given. The relative yields and production cross sections are converted to absolute yields by using the prescription followed in the present work, which has been discussed before. The absolute yields along with the relative ones are also given in the same table. The absolute yields of the asymmetric and symmetric products in the ^{232}Th(γ, f) and ^{238}U(γ, f) reactions at higher energies from Table IV and at lower energies from Refs. [26,44] are plotted in Fig. 8, whereas the P/V ratios are plotted in Fig. 9.

It can be seen from Fig. 8 that with the increase of excitation energy, the yields of asymmetric product decreases systematically in the ^{232}Th(γ, f) reaction, but very slowly in the ^{238}U(γ, f) reaction. On the other hand, the yield of symmetric products in both the ^{232}Th(γ, f) and ^{238}U(γ, f) reactions increases sharply with the increase of excitation energy. The P/V ratio decreases accordingly with the increase of excitation energy as shown in Fig. 9. However, the increase trend of symmetric product yields and the decrease trend of P/V ratio is sharper in both the ^{232}Th(γ, f) and the ^{238}U(γ, f) reactions

TABLE IV. Average excitation energy of compound nucleus ($\langle E^*(E_e)\rangle$), absolute or relative (R) yields (%), and production cross sections (σ) of asymmetric and symmetric products (mb) as well as the P/V ratio in the ^{232}Th(γ, f) and ^{238}U(γ, f) reactions.

E_γ (MeV)	$\langle E^*(E_e)\rangle$ (MeV)	Nuclide	Asymmetric[a]	Nuclide	Symmetric[a]	P/V ratio	References
^{232}Th(γ, f)							
80	22.5	^{138}Cs	5.901 ± 0.554	^{115g}Cd	1.290 ± 0.203	4.57 ± 0.83	[24]
300	65.6	^{91}Sr	5.5 (R), 4.284	^{112}Ag	4.6 (R), 3.582	1.20	[15]
500	141	^{91}Sr	5.5 (R), 3.784	^{112}Ag	6.2 (R), 4.266	0.89	[15]
700	171	^{91}Sr	5.5 (R), 3.355	^{112}Ag	6.8 (R), 4.148	0.81	[15]
900	197	^{91}Sr	5.5 (R), 2.965	^{112}Ag	7.3 (R), 4.043	0.73	[15]
		^{140}Ba	6.0 (R), 3.234	^{112}Ag	7.3 (R), 4.043	0.77	
1100	217	^{91}Sr	5.5 (R), 2.891	^{112}Ag	8.3 (R), 4.362	0.67	[15]
		^{140}Ba	6.2 (R), 3.259	^{112}Ag	8.3 (R), 4.362	0.73	
2500	292	^{91}Sr	2.786 ± 0.176	^{112}Ag	3.857 ± 0.206	0.72 ± 0.06	this work
		^{89}Rb	2.856 ± 0.099	^{112}Ag	3.857 ± 0.206	0.74 ± 0.05	
		^{140}Ba	2.940 ± 0.267	^{112}Ag	3.857 ± 0.206	0.76 ± 0.08	
		^{91}Sr	2.786 ± 0.176	^{113}Ag	4.218 ± 0.233	0.66 ± 0.06	
		^{89}Rb	2.856 ± 0.101	^{113}Ag	4.218 ± 0.233	0.68 ± 0.04	
		^{140}Ba	2.940 ± 0.267	^{113}Ag	4.218 ± 0.233	0.70 ± 0.07	
3500	315	asy	63.0 ± 9.45 (σ)	sym	74.50 ± 11.17 (σ)	0.84 ± 0.17	[21]
^{238}U(γ, f)							
100	22.4	^{97}Zr	5.8 ± 0.2	^{117}Cd	0.69 ± 0.02	8.41 ± 0.38	[27]
		^{97}Zr	5.8 ± 0.2	^{115}Cd	0.718 ± 0.03	8.08 ± 0.44	
		^{97}Zr	5.8 ± 0.2	^{113}Ag	0.77 ± 0.04	7.53 ± 0.47	
		^{97}Zr	5.8 ± 0.2	^{112}Ag	0.71 ± 0.04	8.17 ± 0.54	
300	61.3	^{140}Ba	4.8 ± 0.2	^{117}Cd	1.04 ± 0.04	4.62 ± 0.26	[27]
		^{140}Ba	4.8 ± 0.2	^{115}Cd	1.35 ± 0.054	3.56 ± 0.21	
		^{140}Ba	4.8 ± 0.2	^{113}Ag	1.21 ± 0.06	3.97 ± 0.26	
		^{140}Ba	4.8 ± 0.2	^{112}Ag	1.14 ± 0.08	4.21 ± 0.34	
		^{97}Zr	7.0 (R), 5.698	^{112}Ag	1.9 (R), 1.547	3.4	[15]
500	112.6	^{97}Zr	5.2 (R), 4.826	^{112}Ag	2.6 (R), 2.413	2.5	[15]
700	138.8	^{97}Zr	6.6 (R), 5.075	^{112}Ag	3.3 (R), 2.538	2.0	[15]
900	156	^{97}Zr	6.3 (R), 4.593	^{112}Ag	3.8 (R), 2.770	1.7	[15]
1000	162.8	$A = 137$	4.290 ± 0.196 (R)	$A = 117$	1.98 (R), 2.185	2.17 ± 0.14	[32]
		$A = 137$	5.093 ± 0.225	$A = 120$	1.8 (R), 2.07	2.38 ± 0.15	
1100	168.9	^{97}Zr	6.8 (R), 4.590	^{112}Ag	4.2 (R), 2.835	1.5	[15]
1500	188.9	^{140}Ba	2400 ± 800 (σ)	^{112}Ag	880 ± 300 (σ)	2.73 ± 1.30	[31]
			7.200 ± 2.400		2.640 ± 0.900		
1800	200	$A = 98$	3.370 ± 0.217 (R)	$A = 117$	0.954 ± 0.110 (R)	3.53 ± 0.47	[33]
			5.321 ± 0.342		1.506 ± 0.174		
			3.370 ± 0.217 (R)		1.340 ± 0.101 (R)		
		$A = 98$	5.321 ± 0.342	$A = 112$	2.116 ± 0.159	2.51 ± 0.25	
2000	206.3	$A = 97$	3.600 ± 0.299 (R)	$A = 116$	1.040 ± 0.093 (R)	3.46 ± 0.42	[33]
			4.842 ± 0.402		1.399 ± 0.125		
			3.600 ± 0.299 (R)		1.540 ± 0.136 (R)		
		$A = 97$	4.842 ± 0.402	$A = 111$	2.071 ± 0.183	2.34 ± 0.28	
3000	230.8	^{99}Mo	1380 ± 400 (σ)	^{112}Ag	490 ± 150 (σ)	2.82 ± 1.23	[31]
			4.140 ± 1.200		1.470 ± 0.480		
			1150 ± 250 (σ)		490 ± 160 (σ)		
		^{133}I	3.450 ± 0.600	^{112}Ag	1.470 ± 0.480	2.35 ± 0.87	
			1050 ± 200 (σ)		490 ± 160 (σ)		
		^{140}Ba	3.150 ± 0.750	^{112}Ag	1.470 ± 0.480	2.14 ± 0.87	
3500	240.6	asy	170.8 ± 25.6 (σ)	sym	79.3 ± 11.9 (σ)	2.16 ± 0.40	[42]
		^{95}Zr + ^{131}I	4.851 ± 0.654	^{117}Cd	1.754 ± 0.088	2.77 ± 0.40	
		^{95}Zr + ^{131}I	4.851 ± 0.654	^{115}Cd	2.083 ± 0.154	2.33 ± 0.36	
		^{95}Zr + ^{131}I	4.851 ± 0.654	^{113}Ag	2.237 ± 0.216	2.17 ± 0.36	
		^{95}Zr + ^{131}I	4.851 ± 0.654	^{112}Ag	2.231 ± 0.223	2.17 ± 0.37	

[a]In columns 3 and 5, the cross section (mb) is mentioned as σ and relative fission yield (%) is marked with R. Rest are absolute fission yields (%).

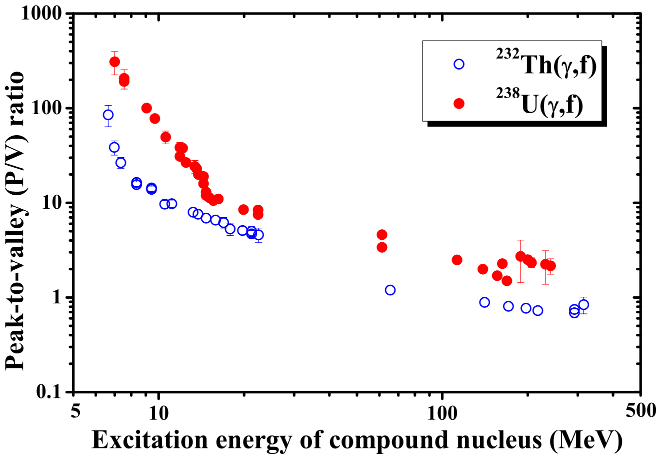

FIG. 9. The peak-to-valley (P/V) ratio as a function of excitation energy of compound nucleus in the ^{232}Th(γ, f) and ^{238}U(γ, f) reactions.

up to the excitation energy of 8.45 MeV ($E_e = 11-12$ MeV). Thereafter, the increase trend with the excitation energy is slow in both reactions. This is because the excitation energy within the bremsstrahlung end-point energy of 11–12 MeV corresponds to the excitation energy of about 8.45 MeV, which is close to the neutron binding energy. Above the neutron binding energy, i.e., above the excitation energy of 8.45 MeV, the second chance of fission starts where the fission occurs from the residual nucleus at lower excitation energy. The number of emitted prefission neutrons also increases with the excitation energy. Thereby, the small part of total excitation energy will be available in the fission degrees of freedom as the intrinsic excitation energy. This causes the slow increase in the yield of symmetric fission products resulting in the slow decrease in the P/V ratio with the increase of excitation energy. Besides this, it can be seen from Figs. 8 and 9 that the yield of symmetric products is always higher and the P/V ratio is always lower in the ^{232}Th(γ, f) reaction than those of the ^{238}U(γ, f) reaction. This observation is due to the different type of potential barrier for the fissioning nucleus ^{232}Th* compared to ^{238}U*, which was shown by Möller [91] in their calculation of saddle point configurations against the mass asymmetric deformation. This has been proved by Yoneama *et al.* [92] using electrofission, i.e., the virtual photon-induced fission of ^{232}Th. As mentioned by them [92], the outer barrier in ^{232}Th splits into two barriers with heights of 6.5 and 5.7 MeV separated by a shallow minimum with a bottom at 5.4 MeV. They have also shown that the barrier height changes for the different vibrational states. The calculation of saddle point configurations against the mass asymmetric deformation by Möller [91] showed a different type of potential barrier for ^{232}Th compared to ^{238}U. Thus, the observation of a triple humped mass distribution from the present and earlier work [13–26] in the bremsstrahlung-induced fission of ^{232}Th compared to that of ^{238}U [27–44] is due to a different type of potential barrier.

V. CONCLUSIONS

(i) The yields of fission products within the mass range of 77–153 in the 2.5-GeV bremsstrahlung-induced fission of ^{232}Th were determined for the first time by using an off-line γ-ray spectrometric technique. Even at the high bremsstrahlung end-point energy of 2.5 GeV, the mass-yield distribution in the ^{232}Th(γ, f) reaction is triple humped, unlike the mass-yield distribution of the ^{238}U(γ, f) reaction is double humped.

(ii) The nuclear structure such as the effect of shell closure proximity and even-odd effect decrease very much at the higher excitation energy. In the ^{232}Th(γ, f) reaction, the yield of fission products for $A = 133-134$ remains almost constant or decreases very little with the increase of excitation energy, whereas those for $A = 143-144$ decreases significantly. This is due to the different roles of standard I and II asymmetric modes of fission depending on the presence of a shell in one or both complementary fragments.

(iii) In both the ^{232}Th(γ, f) and the ^{238}U(γ, f) reactions, the yield of asymmetric products decreases marginally, whereas the yield of symmetric products increases sharply with the excitation energy. However, the increase trend is more pronounced up to the excitation energy of 8.5 MeV ($E_e = 11 - 12$ MeV). Thereafter, it increases slowly due to more prefission neutron emission and the multichance fission probability. Thus, the peak-to-valley (P/V) ratio decreases accordingly with the increase of excitation energy.

(iv) At the same excitation energy, the yield of symmetric products is always higher and thus the P/V ratio is lower in the ^{232}Th(γ, f) reaction than those in the ^{238}U(γ, f) reaction. This is due to the third peak in the mass-yield distribution of the ^{232}Th(γ, f) reaction resulting from a different potential barrier in the fissioning nucleus ^{232}Th* compared to ^{238}U*.

(v) In the ^{232}Th(γ, f) reaction, the $\langle A_H \rangle$ value decreases and the $\langle A_L \rangle$ value increases with the increase of excitation energy. This is favored the standard II mode rather than the standard I mode of fission. The $\langle A_H \rangle$ value in the ^{238}U(γ, f) reaction is lower than that in the ^{232}Th(γ, f) reaction and remains almost constant or slightly decreases with the increase of excitation energy. This is favored the standard I mode rather than the standard II mode of fission in the ^{238}U(γ, f) reaction. The $\langle A_L \rangle$ value in the ^{238}U(γ, f) reaction is always higher than that in the ^{232}Th(γ, f) reaction and systematically decreases with the increase of excitation energy to conserve the mass of the fissioning system.

(vi) In the bremsstrahlung- and neutron-induced fission of ^{232}Th and ^{238}U, the values of postfission average number of neutrons ($\langle \upsilon \rangle_{\text{expt}}$) increase with the increase of excitation energy. However, at the same excitation energy, the values of $\langle \upsilon \rangle_{\text{expt}}$ in the ^{238}U(γ, f) and ^{238}U(n, f) reactions are always higher than those in the ^{232}Th(γ, f) and ^{232}Th(n, f) reactions due to the increase in mass and fissility parameters.

ACKNOWLEDGMENTS

The authors express their sincere thanks to the staff of the PAL for the excellent operation of the electron linac and their support during the experiment. This research was partly supported by the Institutional Activity Program of KAERI, 2017, by the National Research Foundation of Korea through a grant provided by the Ministry of Science and ICT (Grant No. NRF-2017R1D1A1B03030484), and by the National R&D Program through the Dong-nam Institute of Radiological and Medical Sciences (Grant No. 50496-2017). One of the authors (H.N.) was supported by the Korean Brain Pool Program (Grant No. 171S-1-3-1786) of Korean Federation of Science and Technology Societies (KOFST).

[1] R. Vandenbosch and J. R. Huizenga, *Nuclear Fission* (Academic, New York, 1973).

[2] C. Wagemans, *The Nuclear Fission Process* (CRC, London, 1990).

[3] Fast Reactors and Accelerator Driven Systems Knowledge Base, IAEA-TECDOC-1319: Thorium fuel utilization: Options and Trends.

[4] A. Nuttin, D. Heuer, A. Biliebaud, R. Brissot, C. Le Brun, E. Liatard, J. M. Loiseaux, L. Mathieu, O. Meplan, E. Merle-Lucotte, H. Nifenecker, F. Perdu, and S. David, Proc. Nucl. Energy **46**, 77 (2005).

[5] T. R. Allen and D. C. Crawford, Science and Technology of Nuclear Installations **2007**, 97486 (2007).

[6] R. K. Sinha and A. Kakodkar, Nucl. Eng. Des. **236**, 683 (2006).

[7] F. Carminati, R. Klapisch, J. P. Revol, J. A. Rubia, and C. Rubia, CERN Report CERN/AT/93-49 (ET) (1993).

[8] C. Rubia, J. A. Rubio, S. Buono, F. Carminati, N. Fietier, J. Galvez, C. Geles, Y. Kadi, R. Klapisch, P. Mandrilion, J. P. Revol, and Ch. Roche, CERN Report CERN/LHC/97-01 (EET) (1997).

[9] C. D. Bowman, AIP Conf. Proc. **346**, 22 (1995).

[10] Accelerator Driven Systems: Energy Generation and Transmutation of Nuclear Waste, Status report, IAEA, Vienna, IAEA Report IAEA-TECDOC-985 (1997).

[11] C. D. Bowman, Annu. Rev. Nucl. Part Sci. **48**, 505 (1998).

[12] K. Oyamatsu, H. Takeuchi, M. Sagisaka, and J. Katakura, J. Nucl. Sci. Technol. **38**, 477 (2001).

[13] D. M. Hiller and D. S. Martin, Jr., Phys. Rev. **90**, 581 (1953).

[14] L. H. Gevaert, R. E. Jervis, S. C. Subbarao, and H. D. Sharma, Can. J. Chem. **48**, 652 (1970).

[15] B. Schrøder, G. Nydahl, and B. Forkman, Nucl. Phys. A **143**, 449 (1970).

[16] A. Chattopadhyay, K. A. Dost, I. Krajbich, and H. D. Sharma, J. Inorg. Nucl. Chem. **35**, 2621 (1973).

[17] J. C. Hogan, A. E. Richardson, J. L. Meason, and H. L. Wright, Phys. Rev. C **16**, 2296 (1977).

[18] W. Gunther, K. Huber, U. Kneissl, H. Krieger, and H. J. Maier, Z. Phys. A **295**, 333 (1980).

[19] M. Piessens, E. Jacobs, S. Pommé, and D. De Frenne, Nucl. Phys. A **556**, 88 (1993).

[20] S. A. Karamian, J. Adam, A. G. Belov, J. J. Carroll, Yu. V. Norseev, V. I. Stegailov, and P. Chaloun, Phys. Rev. C **62**, 024601 (2000).

[21] N. A. Demekhina and G. S. Karapetyan, Phys. At. Nucl. **73**, 24 (2010).

[22] H. Naik, V. T. Nimje, D. Raj, S. V. Suryanarayana, A. Goswami, S. Singh, S. N. Acharya, K. C. Mttal, S. Ganesan, P. Chandrachoodan, V. K. Manchanda, V. Venugopal, and S. Banarjee, Nucl. Phys. A **853**, 1 (2011).

[23] H. Naik, T. N. Nathaniel, A. Goswami, G. N. Kim, M. W. Lee, S. V. Suryanarayana, S. Ganesan, E. A. Kim, M. H. Cho, and K. L. Ramakumar, Phys. Rev. C **85**, 024623 (2012).

[24] H. Naik, A. Goswami, G. N. Kim, M. W. Lee, K. S. Kim, S. V. Suryanarayana, E. A. Kim, S. G. Shin, and M.-H. Cho, Phys. Rev. C **86**, 054607 (2012).

[25] H. Naik, B. S. Shivashankar, H. G. Raj Prakash, D. Raj, G. Sanjeev, N. Karunakara, H. M. Somashekarappa, S. Ganesan, G. N. Kim, and A. Goswami, J. Radioanal. Nucl. Chem. **299**, 127 (2014).

[26] H. Naik, G. N. Kim, R. Schwengner, K. Kim, R. John, R. Massarczyk, A. Junghans, A. Wagner, and A. Goswami, Eur. Phys. J. A **51**, 150 (2015)

[27] R. A. Schmitt and N. Sugarman, Phys. Rev. **95**, 1260 (1954).

[28] H. G. Richter and C. D. Coryell, Phys. Rev. **95**, 1550 (1954).

[29] L. Katz, T. M. Kavanagh, A. G. W. Cameron, E. C. Bailey, and J. W. T. Spinks, Phys. Rev. **99**, 98 (1958).

[30] J. L. Meason and P. K. Kuroda, Phys. Rev. **142**, 691 (1966).

[31] I. R. Willams, C. B. Fulmer, G. F. Dell, and M. J. Engebretson, Phys. Lett. B **26**, 140 (1968).

[32] A. P. Komar, B. A. Bochagov, A. A. Kotov, Yu. N. Ranyuk, G. G. Semenchuk, G. E. Solyakin, and P. V. Sorokin, Sov. J. Nucl. Phys. **10**, 30 (1970).

[33] P. David, J. Debrus, U. Kim, G. Kumbartzki, H. Mommsen, W. Soyez, K. H. Speidel, and G. Stein, Nucl. Phys. A **197**, 163 (1972).

[34] D. Swindle, R. Wright, K. Takahashi, W. H. Rivera, and J. L. Meason, Nucl. Sci. Eng. **52**, 466 (1973).

[35] W. D. James, D. E. Adams, R. A. Sigg, J. T. Harvey, J. L. Meason, J. N. Beck, P. K. Kuroda, H. L.Wright, and J. C. Hogan, J. Inorg. Nucl. Chem. **38**, 1109 (1978).

[36] H. Thierens, D. De Frenne, E. Jacobs, A. De Clercq, P. D'hondt, and A. J. Deruytter, Phys. Rev. C **14**, 1058 (1976).

[37] E. Jacobs, H. Thierens, D. De Frenne, A. De Clercq, P. D'hondt, P. De Gelder, and A. J. Deruytter, Phys. Rev. C **19**, 422 (1979).

[38] A. De Clercq, E. Jacobs, D. De Frenne, H. Thierens, P. D'hondt, and A. J. Deruytter, Phys. Rev. C **13**, 1536 (1976).

[39] E. Jacobs, A. De Clercq, H. Thierens, D. De Frenne, P. D'hondt, P. De Gelder, and A. J. Deruytter, Phys. Rev. C **20**, 2249 (1979).

[40] S. Pommé, E. Jacobs, M. Piessens, D. De Frenne, K. Persyn, K. Govaert, and M.-L. Yoneama, Nucl. Phys. A **572**, 237 (1994).

[41] A. Yamadera, T. Kase, and T. Nakamura, in *Proceedings of the International Conference on Nuclear Data for Science and Technology*, edited by S. Igarasi, Moto, Japan, 1988 (Japan Atomic Energy Research Institute, Tokai, Japan, 1988), p. 1147.

[42] N. A. Demekhina and G. S. Karapetyan, Phys. At. Nucl. **71**, 27 (2008).

[43] A. Göök, M. Chernykh, C. Eekardt, J. Enders, P. von Neumann-Cosel, A. Oberstedt, S. Oberestedt, and A. Richter, Nucl. Phys. A **851**, 1 (2011).

[44] H. Naik, Frédérick Carrel, G. N. Kim, Frédéric Laine, A. Sari, S. Normand, and A. Goswami, Eur. Phys. J. A **49**, 94 (2013).
[45] S. Agostinelli *et al.* (GEANT4 Collaboration), Nucl. Instrum. Methods Phys. Res. A **506**, 250 (2003).
[46] IAEA-EXFOR, Experimental nuclear reaction data. available at http://www-nds.iaea.org/exfor.
[47] J. T. Caldwell, E. J. Dowdy, B. L. Berman, R. A. Alvarez, and P. Meyer, Phys. Rev. C **21**, 1215 (1980).
[48] A. Lepretre, R. Bergere, P. Bourgeois, P. Carlos, J. Fagot, J. L. Fallou, P. Garganne, A. Veyssiere, H. Ries, R. Gobel, U. Kneissl, G. Mank, H. Stroher, W. Wilke, D. Ryckbosch, and J. Jury, Nucl. Phys. A **472**, 533 (1987).
[49] N. Bianchi, A. Deppman, E. De Sanctis, A. Fantoni, P. Levi Sandri, V. Lucherini, V. Muccifora, E. Polli, A. R. Reolon, P. Rossi, A. S. Iljinov, M. V. Mebel, and J. D. T. Arruda-Neto, Phys. Rev. C **48**, 1785 (1993).
[50] J. C. Sanabria, B. L. Berman, C. Cetina, P. L. Cole, G. Feldman, N. R. Kolb, R. E. Pywell, J. M. Vogt, V. G. Nedorezov, A. S. Sudov, and G. Ya. Kezerashvili, Phys. Rev. C **61**, 034604 (2000).
[51] C. Cetina, P. Heimberg, B. L. Berman, W. J. Briscoe, G. Feldman, L. Y. Murphy, H. Crannell, A. Longhi, D. I. Sober, J. C. Sanabria, and G. Ya. Kezerashvili, Phys. Rev. C **65**, 044622 (2002).
[52] Th. Frommhold, F. Steiper, W. Henkel, U. Kneissl, J. Ahrens, R. Beck, J. Peise, M. Schmitz, I. Anthony, J. D. Kellie, S. J. Hall, and G. J. Miller. Z. Phys. A: Hadrons Nucl. **350**, 249 (1994).
[53] H. Ries, U. Kneissl, G. Mank, H. Stroher, W. Wilke, R. Bergere, P. Bourgeois, P. Carlos, J. L. Fallou, P.Garganne, A. Veyssiere, and L. S. Cardman, Phys. Lett. B **139**, 254 (1984).
[54] S. Bjornholm and J. E. Lynn, Rev. Mod. Phys. **52**, 725 (1980).
[55] NuDat 2.6, National Nuclear Data Center, Brookhaven National Laboratory, updated 2011, available at http://www.nndc.bnl.gov/.
[56] E. Browne and R. B. Firestone, in *Table of Radioactive Isotopes*, edited by V. S. Shirley (Wiley, New York, 1986); R. B. Firestone and L. P. Ekstrom, in *Table of Radioactive Isotopes*, Version 2.1 (2004), available at http://ie.lbl.gov/toi/index.asp.
[57] J. Blachot and C. Fiche, Ann. Phys. Suppl. **6**, 3 (1981).
[58] A. C. Wahl, At. Data Nucl. Data Tables **39**, 1 (1988).
[59] K. Persyn, E. Jacobs, S. Pommé, D. De Frenne, K. Govaert, and M.-L. Yoneama, Nucl. Phys. A **620**, 171 (1997).
[60] S. Pommé, E. Jacobs, K. Persyn, D. De Frenne, K. Govaert, and M. L. Yoneama, Nucl. Phys. A **560**, 689 (1993).
[61] D. De Frenne, H. Thierens, B. Proot, E. Jacobs, P. De Gelder, A. De Clercq, and W. Westmeier, Phys. Rev. C **26**, 1356 (1982).
[62] H. Umezawa, S. Baba, and H. Baba, Nucl. Phys. A **160**, 65 (1971).
[63] N. Sugarman and A. Turkevich, in *Radiochemical Studies: The Fission Product*, edited by C. D. Coryell and N. Sugarman (McGraw-Hill, New York, 1951), Vol. 3, p. 1396.
[64] M. Strecker, R. Wien, P. Plischke, and W. Scobel, Phys. Rev. C **41**, 2172 (1990).
[65] A. Deppman, E. Andrade-II, V. Guimaraes, G. S. Karapetyan, and N. A. Demekhina, Phys. Rev. C **87**, 054604 (2013).
[66] A. Deppman, S. B. Duarte, G. Silva, O. A. P Tavares, S. Anéfalos, J. D. T. Arruda-Neto, and T. E. Rodrigues, J. Phys. G: Nucl. Part. Phys. **30**, 1991 (2004).
[67] I. V. Ryzhov, S. G. Yavshits, G. A. Tutin, N. V. Kovalev, A. V. Saulski, N. A. Kudryashev, M. S. Onegin, L. A. Vaishnene, Yu. A. Gavrikov, O. T. Grudzevich, V. D. Simutkin, S. Pomp, J. Blomgren, M. Österlund, P. Andersson, R. Bevilacqua, J. P. Meulders, and R. Prieels, Phys. Rev. C **83**, 054603 (2011).
[68] C. M. Zöller, A. Gavron, J. P. Lestone, M. Mutterer, J. P. Theobald, A. S. Iljinov, and M. V. Mebel, in *Proceedings of the Seminar on Fission*, edited by C. Wagemans, J. Wagemans, and P. D'hondt (Pont d'Oye, Haby-la-Neuve, Belgium, 1995), Report EUR 16295 EN.
[69] U. Brossa, S. Grossmann, and A. Muller, Phys. Rep. **197**, 167 (1990).
[70] B. D. Wilkins, E. P. Steinberg, and R. R. Chasman, Phys. Rev. C **14**, 1832 (1976).
[71] K.-H. Schmidt, B. Jurado, C. Amouroux, and C. Schmitt, Nucl. Data Sheets **131**, 107 (2016).
[72] R. E. Howe, Nucl. Sci. Eng. **86**, 157 (1984).
[73] V. V. Malinovskiy, V. G. Vorob'yova, B. D. Kuz'minov, V. M. Piksaikin, N. N. Semyonova, V. S. Valyavkin, and S. M. Solov'yov, Atomnaya Energiya **54**, 209 (1983).
[74] J. Frehaut, R. Bois, and A. Bertin, in *Proceedings of International Conference on Nuclear Data for Science and Technology*, edited by K. H. Bockhoff (Antwerp, Belgium, 1982), pp. 78–84.
[75] H. Naik, S. Mukherji, S. V. Suryanarayana, K. C. Jagadeesan, S. V. Thakare, and S. C. Sharm, Nucl. Phys. A **952**, 100 (2016).
[76] H. Naik, R. Crasta, S. V. Suryanarayana, P. M. Prajapati, V. K. Mulik, B. S. Shivasankar, K. C. Jagadeesan, S. V. Thakare, S. C. Sharma, and A. Goswami, Eur. Phys. J. A **50**, 144 (2014).
[77] L. E. Glendenin, J. E. Gindler, I. Ahmad, D. J. Henderson, and J. W. Meadows, Phys. Rev. C **22**, 152 (1980).
[78] K. M. Broom, Phys. Rev. **133**, B874 (1964).
[79] J. Frehaut (private communication).
[80] B. Nurpeisov, K. E. Volodin, V. G. Nesterov, L. I. Prokhorova, G. N. Smirenkin, and Yu. N. Turchin, Atomnaya Energiya **39**, 199 (1975).
[81] H. Naik, S. Mukerji, R. Crasta, S. V. Suryanarayana, S. C. Sharma, and A. Goswami, Nucl. Phys. A **941**, 16 (2015).
[82] H. Naik, V. K. Mulik, P. M. Prajapati, B. S. Shivasankar, S. V. Suryanarayana, K. C. Jagadeesan, S. V. Thakare, S. C. Sharma, and A. Goswami, Nucl. Phys. A **913**, 185 (2013).
[83] Z. Li, X. Wang, K. Jing, A. Cui, D. Liu, S. Su, P. Tang, T. Chih, S. Zhang, and J. Gao, Radiochim. Acta **64**, 95 (1994).
[84] L. Ze, Z. Chunhua, L. Conggui, W. Xiuzhi, Q. Limkun, C. Anzhi, L. Huijung, Z. Sujing, L. Yonghui, J. Changxin, L. Daming, T. Peija, M. Jiangchen, and J. Kixing, High Energy Phys. J. Nucl. Phys. **7**, 97 (1985) (in Chinese).
[85] S. Nagy, K. F. Flynn, J. E. Gindler, J. W. Meadows, and L. E. Glendenin, Phys. Rev. C **17**, 163 (1978).
[86] T. C. Chapman, G. A. Anzelon, G. C. Spitale, and D. R. Nethaway, Phys. Rev. C **17**, 1089 (1978).
[87] T. Harvey, D. E. Adams, W. D. James, J. N. Beck, J. L. Meason, and P. K. Kuroda, J. Inorg. Nucl. Chem. **37**, 2243 (1975).
[88] J. Blachot, L. C. Carraz, P. Cavalini, C. Chauvin, A. Ferrieu, and A. Moussa, J. Inorg. Nucl. Chem. **36**, 495 (1974).
[89] D. E. Adams, W. D. James, J. N. Beck, and P. K. Kuroda, J. Inorg. Nucl. Chem. **37**, 419 (1975).
[90] J. K. Tuli, Nuclear Wallet Cards, National Nuclear Data Center, Brookhaven National Laboratory, Uption, New York, USA (2011), http://www.nndc.bnl.gov.
[91] P. Moller, Nucl. Phys. A **192**, 529 (1972).
[92] M. L. Yoneama, E. Jacobs, J. D. T. Arruda-Neto, B. S. Bhandari, D. De Frenne, S. Pommé, K. Persyn, and K. Govaert, Nucl. Phys. A **604**, 263 (1996).